MBOC: The New Optimized Spreading Modulation Recommended for GALILEO L1 OS and GPS L1C

Guenter W. Hein, Jose-Angel Avila-Rodriguez, Stefan Wallner, Anthony R. Pratt, John Owen, Jean-Luc Issler

John W. Betz, Chris J. Hegarty, Lt Sean Lenahan, Joseph J. Rushanan, Andrea L. Kraay, Thomas A. Stansell

Guenter W. Hein is Full Professor and Director of the Institute of Geodesy and Navigation at the University FAF Munich. He is responsible for research and teaching in the fields of high-precision GNSS positioning and navigation, physical geodesy and satellite methods. He has been working in the field of GPS since 1984 and is author of numerous papers on kinematic positioning and navigation as well as sensor integration. In 2002 he received the prestigious “Johannes Kepler Award“ from the US Institute of Navigation (ION) for ”sustained and significant contributions to satellite navigation“. Presently he is heavily involved in the GALILEO program.

John W. Betz is a Fellow of The MITRE Corporation. His PhD in Electrical and Computer Engineering is from Northeastern University. He contributed to the design of the GPS M-code signal, led the Modulation and Acquisition Design Team, and developed the binary offset carrier (BOC) modulation. He has contributed to many aspects of GNSS engineering, and has participated in international efforts to achieve compatibility and interoperability between GPS and other satellite navigation systems. He received the ION Burka Award in 2001, and is a member of the US Air Force Scientific Advisory Board, and a Fellow of the ION.

José-Ángel Ávila-Rodríguez is research associate at the Institute of Geodesy and Navigation at the University of the Federal Armed Forces Munich. He is responsible for research activities on GNSS signals, including BOC, BCS, and MBCS modulations. He is involved in the GALILEO program, in which he supports the European Space Agency, the European Commission, and the GALILEO Joint Undertaking, through the GALILEO Signal Task Force. He studied at the Technical Universities of Madrid, Spain, and Vienna, Austria, and has an M.S. in electrical engineering. His major areas of interest include the GALILEO signal structure, GNSS receiver design and performance, and GALILEO codes.

Christopher J. Hegarty is a Senior Principal Engineer with The MITRE Corporation's Center for Advanced Aviation System Development. He received a D.Sc. in Electrical Engineering from The George Washington University. He is a member of RTCA's Program Management Committee and co-chair of RTCA Special Committee 159. He was a recipient of the 1998 ION Early Achievement Award and the 2005 Johannes Kepler Award. He currently serves the ION as Editor of *NAVIGATION: Journal of the Institute of Navigation* and as Eastern Region Vice President.

Stefan Wallner studied at the Technical University of Munich and graduated in 2003 with a Diploma in Techno-Mathematics. He is now research associate at the Institute of Geodesy and Navigation at the University of the Federal Armed Forces Germany in Munich. His main topics of interests can be denoted as the Spreading Codes and the Signal Structure of GALILEO.

Anthony R. Pratt graduated with a B.Sc. and Ph.D. in Electrical and Electronic Engineering from Birmingham University, UK. He joined the teaching staff at Loughborough University, UK in 1967 and remained until 1980. He held visiting professorships at Yale University, IIT New Delhi and at the University of Copenhagen. In 1980, he joined Navstar Ltd, as Technical Director. In 1991, he joined Peek acting in several roles including running Tollstar, a road tolling opportunity. He left Peek in 1997 and joined Navstar Systems Ltd as Technical Consultant. He is now Technical Director (GPS) with Parthus. He is also a Special Professor at the IESSG, University of Nottingham, UK. He acts as Consultant to the UK Government in the development of GALILEO Satellite System.

Lt Lawrence S. Lenahan is the L1C Project Military Co-Chair and works for the GPS Joint Program Office in its Engineering and Advanced Technology Branch, after 3 years with the 2d Space Operations Squadron as its

Engineer On-Call for Spacecraft Anomalies. Lt Lenahan received a B.S. degree from the United States Air Force Academy in Astronautical Engineering and is currently a member of ION and AIAA.

John I. R. Owen is Leader of Navigation Systems, Air Systems Department, DSTL. He is a DSTL Senior Fellow, a Fellow of the Royal Institute of Navigation. He gained a BSc (Hons) in Electrical and Electronic Engineering, Loughborough University, and joined the Royal Aircraft Establishment to research aspects of aircraft antennas. He helped develop the first GPS adaptive antenna system. He moved to the satellite navigation research group in 1982 and was responsible for the technical development of GPS receivers, antenna systems and simulators in the UK. Following the formation of DERA, he was responsible for the satellite navigation aspects of UK MOD's research programmes for aircraft and missiles. He is technical adviser to UK Government Departments for GPS and the European GALILEO programme, where he is active on the Signal Working Group, the Security Board and the European Space Agency Programme Board for Navigation. He chaired the ICAO Global Navigation Satellite Systems spectrum subgroup.

Jean-Luc Issler is head of the Transmission Techniques and signal processing department of CNES, whose main tasks are signal processing, air interfaces and equipments in Radionavigation, TT&C, Image telemetry, propagation and spectrum survey. With DRAST and DGA, he represents France in the GALILEO Signal Task Force of the European Commission. Lionel Ries, Antoine DeLatour and Laurent Lestarquit, from his team, were deeply involved in the design of CBOC, one of the recommended optimized GALILEO OS signal. He is involved in the development of several spaceborne receivers in Europe. He received the "Astronautical Prize" from the "Association Aeronautique et Astronautique de France" for his involvement in the GALILEO frequency choice and signal design

Joseph J. Rushanan is a Principal Mathematician in the Signal Processing Section of the MITRE Corporation. His expertise includes discrete mathematics, including binary sequences, and general security engineering. He has a BS and MS in 1982 from the Ohio State University and a Ph. D. from the California Institute of Technology in 1986, all in mathematics. He has been with MITRE since 1986.

Andrea L. Kraay received a B.S. in Electrical Engineering from George Mason University in 1999, a S.M. and Engineer's degree in Electrical Engineering and Computer Science from the Massachusetts Institute of Technology and Woods Hole Oceanographic Institution in 2003. From 1997 until 2000 she worked as an engineer for Digital Systems Resources, Inc. in Fairfax, Virginia developing and testing algorithms for underwater target detection and classification. From 2000 to 2003 she was a research assistant at MIT's Ocean Engineering Acoustics Laboratory in Cambridge, Massachusetts where she conducted research in reduced rank adaptive array processing techniques for interference cancellation and improved power estimation in non-stationary environments. She is currently a senior engineer in the Signal Processing Group at the MITRE Corporation in Bedford, Massachusetts working in radar, navigation, and communications system design.

Tom Stansell heads Stansell Consulting, after 8 years with the Johns Hopkins Applied Physics Laboratory, 25 years with Magnavox (Staff VP), and 5 years with Leica (VP), pioneering Transit and GPS navigation and survey products. He served on the WAAS Independent Review Board (2000); led technical development of the GPS L2C signal (2001); and is coordinator of the GPS L1C project. ION and other awards: Weems Award (1996), Fellow (1999), Kershner (PLANS-2000), GPS JPO Navstar Award (2002), and Johannes Kepler (2003). He was technical chair ('84, '86, and '88) and general chair ('94, '96, and '98) of PLANS conferences, technical chair of ION GPS-91, and general chair of ION GPS-92. He also is Western Regional VP of the ION.

ABSTRACT

This paper describes the Multiplexed Binary Offset Carrier (MBOC) spreading modulation that has been recommended by the GPS-GALILEO Working Group on Interoperability and Compatibility. The MBOC(6,1,1/11) power spectral density is a mixture of BOC(1,1) spectrum and BOC(6,1) spectrum, that would be used by GALILEO for its Open Service (OS) signal at L1 frequency, and also by GPS for its modernized L1 Civil (L1C) signal. A number of different time waveforms can produce the MBOC(6,1,1/11) spectrum, allowing flexibility in implementation, although interoperable waveforms remains an objective for GALILEO and GPS. The time-multiplexed BOC (TMBOC) implementation interlaces BOC(6,1) and BOC(1,1) spreading symbols in a regular pattern, whereas composite BOC (CBOC) uses multilevel spreading symbols formed from the weighted sum of BOC(1,1) and BOC(6,1) spreading symbols, interplexed to form a constant modulus composite signal. This paper provides information on the history, motivation, and construction of MBOC signals. It then shows various performance characteristics, and summarizes their status in GALILEO and GPS signal design.

INTRODUCTION

On June 26th, 2004, the United States of America and the European Community established the "Agreement on the Promotion, Provision and Use of GALILEO and GPS Satellite-Based Navigation Systems and Related Applications" [1]. One aspect of the Agreement was to adopt a common baseline signal to be transmitted in the future by GALILEO and GPS at the L1 center frequency of 1575.42 MHz. Although the Agreement established BOC(1,1) as the baseline for GALILEO L1 OS and GPS future L1C signals, it also stated that the Parties shall work together toward achieving optimization of that modulation for their respective systems, within the constraints of the Agreement.

A recent joint design activity involving experts from the United States and Europe has produced a recommended optimized spreading modulation for the L1C signal and the GALILEO L1 OS signal [2, 3]. The spreading modulation design places a small amount of additional power at higher frequencies in order to improve signal tracking performance. This paper describes the spreading modulation's power spectral density (PSD), as well as alternative spreading time series and their autocorrelation functions. In addition, various measures are used to assess the performance benefits of the optimized modulation compared to those of other modulations. The status and way ahead are then summarized.

MBOC POWER SPECTRAL DENSITY

The spreading modulation for the legacy civil signal at 1575.42 MHz, the GPS C/A code, is based on binary phase shift keyed signal with a rectangular pulse shape and a spreading code chip rate of 1.023 MHz, denoted BPSK-R(1). While very good performance can be obtained with the C/A code signal, it has been recognized that better performance can be obtained using spreading modulations that provide more power at high frequencies away from the center frequency. Binary offset carrier (BOC) spreading modulations [4] are one way to accomplish this, and a BOC(1,1) spreading modulation was selected as the baseline for the future GALILEO L1 OS and GPS L1C signals. Fig. 1 shows BOC(1,1)'s resulting increase in higher frequency power, compared to BPSK-R(1).

The multiplexed binary offset carrier (MBOC) PSD recommended in [2, 3] is the PSD of the entire signal (pilot and data components together), denoted MBOC(6,1,1/11), and given by

$$G_{Signal}(f) = \frac{10}{11} G_{BOC(1,1)}(f) + \frac{1}{11} G_{BOC(6,1)}(f) \qquad (1)$$

where $G_{BOC(m,n)}(f)$ is the unit-power PSD of a sine-phased BOC spreading modulation as defined in [4]. The selection of this PSD and identification of practical ways to produce time waveforms that implement it are based on extensive work by many individuals. Some of these foundational references are listed in [4 -11].

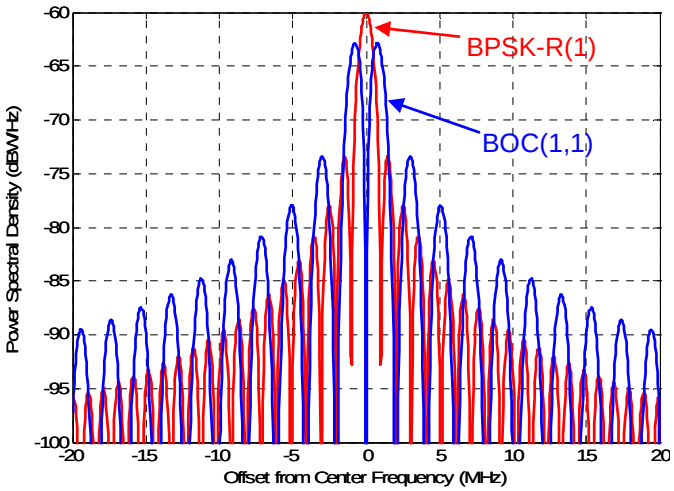

Fig. 1. Unit Power PSD of BPSK-R(1) and BOC(1,1) Spreading Modulations, Showing BOC(1,1)'s Additional Power at Higher Frequencies

MBOC(6,1,1/11)'s resulting increase in higher frequency power, compared to that of BOC(1,1), is evident in Fig. 2. As will be seen, the improvement in high frequency power for signal tracking can be even greater than what is shown in Fig. 2 by placing all or most of the BOC(6,1) symbols, which provide the additional high frequency power, in the pilot component of the signal.

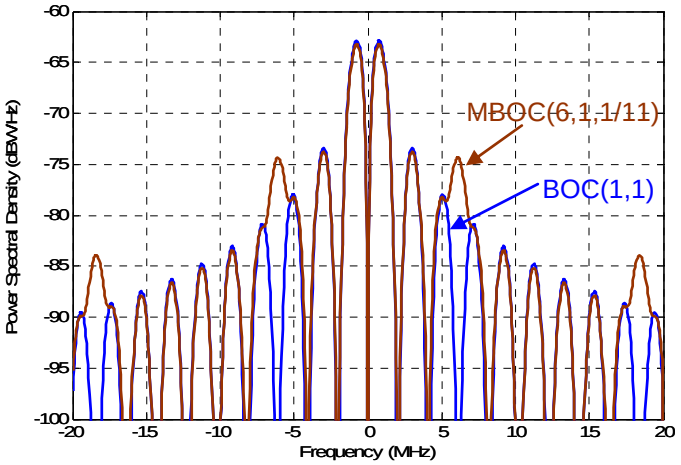

Fig. 2. Unit Power PSD of BOC(1,1) and MBOC(6,1,1/11) Spreading Modulations, Showing MBOC(6,1,1/11)'s Additional Power at Higher Frequencies

The recommended MBOC(6,1,1/11) is a specific case of more general spreading modulations that have been studied extensively. It was selected to meet technical constraints in the Agreement [1], to retain a high degree of interoperability with receivers that might use BOC(1,1), and to facilitate implementation in satellites and receivers.

SPREADING TIME SERIES AND AUTOCORRELATION FUNCTION

A variety of time waveforms can be used to produce the MBOC(6,1,1/11) PSD described in (1). Two fundamentally different approaches, time-multiplexed BOC (TMBOC) and composite BOC (CBOC), are described in this section, along with various applications of each approach.

Denote a baseband spread spectrum waveform by

$$s(t) = \sum_{k=-\infty}^{\infty} a_k g_k(t - kT_c) \tag{2}$$

where the $\{a_k\}$ take on the values ± 1 as determined by the combination of spreading code chip, any data message symbol, and any overlay code bit, T_c is the spreading code chip rate, and $\{g_k(t)\}$ are spreading symbols expressed in a general enough form so that they can be different for different values of k. (Clearly, more general versions of (2) could employ complex-valued $\{a_k\}$ and $g_k(t)$ to achieve higher-order phase modulations.)

Define the spreading time series as the deterministic time series produced with the chip values formed by the combination of the spreading code bits, any data message symbols, and any overlay code or other secondary code. For example, a BPSK-R spreading time series takes on the constant value of unity, while a BOC time series is merely the repetition of identical BOC spreading symbols. The most general case corresponds to BCS signals, whose time series is given by a vector s as shown in [8, 9]. According to this the spreading time series of BPSK-R in (2) is defined as

$$s(t) = \sum_{k=-\infty}^{\infty} g_k(t - kT_c) \tag{3}$$

TMBOC Implementation

In a TMBOC spreading time series, different BOC spreading symbols are used for different values of k, in either a deterministic or periodic pattern. To produce a MBOC(6,1,1/11) spectrum, the spreading symbols used are BOC(1,1) spreading symbols denoted $g_{BOC(1,1)}(t)$ and and BOC(6,1) spreading symbols denoted $g_{BOC(6,1)}(t)$, with

$$g_{BOC(1,1)}(t) = \begin{cases} \mathrm{sgn}[\sin(2\pi t / T_c)] & 0 \le t \le T_c \\ 0 & \text{elsewhere} \end{cases} \tag{4}$$

and defined by

$$g_{BOC(6,1)}(t) = \begin{cases} \mathrm{sgn}[\sin(12\pi t / T_c)] & 0 \le t \le T_c \\ 0 & \text{elsewhere} \end{cases} \tag{5}$$

Since the pilot and data components of a signal can be formed using different spreading time series, and the total signal power can be divided differently between the pilot and data components, many different TMBOC-based implementations are possible.

A candidate TMBOC implementation for a signal with 75% power on the pilot component and 25% power on the data component, could use all BOC(1,1) spreading symbols on the data component, since data demodulation does not benefit from the higher frequency contributions of the BOC(6,1), and pilot component whose spreading time series comprises 29/33 BOC(1,1) spreading symbols and 4/33 BOC(6,1) spreading symbols. This design places all of the higher frequency contributions in the pilot component, providing the greatest possible benefit to signal tracking when only the pilot channel is used to this purpose, while yielding the PSDs

$$\begin{aligned} G_{Pilot}(f) &= \frac{29}{33} G_{BOC(1,1)}(f) + \frac{4}{33} G_{BOC(6,1)}(f) \\ G_{Data}(f) &= G_{BOC(1,1)}(f) \\ G_{MBOC(6,1,1/11)}(f) &= \frac{3}{4} G_{Pilot}(f) + \frac{1}{4} G_{Data}(f) \\ &= \frac{10}{11} G_{BOC(1,1)}(f) + \frac{1}{11} G_{BOC(6,1)}(f) \end{aligned} \tag{6}$$

Fig. 3 next shows an example of this implementation, with the BOC(6,1) spreading symbols in locations 1, 5, 7, and 30 of each 33 spreading symbol locations. This pattern could be

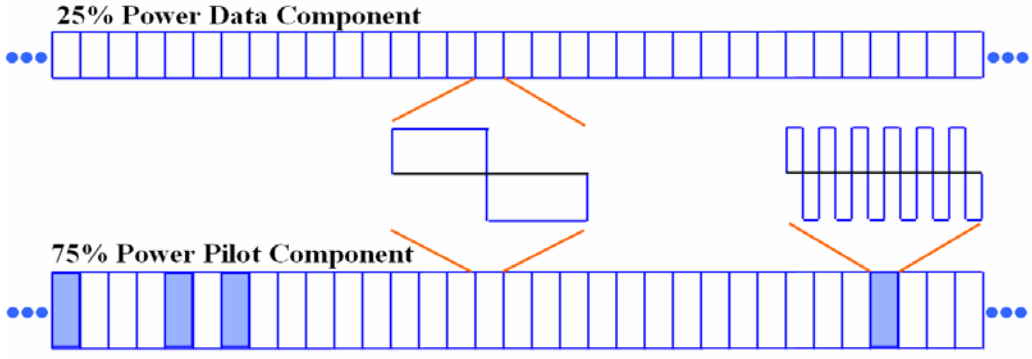

Fig. 3. Example of TMBOC(6,1,4/33) Spreading Time Series, with All BOC(6,1) Spreading Symbols in the 75% Pilot Power Component

repeated 310 times if the spreading code length is 10230, or 124 times if the spreading code length is 4092.

For a signal with 50%/50% power split between pilot and carrier component, a candidate TMBOC implementation would be to use all BOC(1,1) spreading symbols on the data component, and 2/11 BOC(6,1) spreading symbols on the pilot, yielding the PSDs

$$\begin{aligned} G_{Pilot}(f) &= \frac{9}{11}G_{BOC(1,1)}(f) + \frac{2}{11}G_{BOC(6,1)}(f) \\ G_{Data}(f) &= G_{BOC(1,1)}(f) \\ G_{MBOC(6,1,1/11)}(f) &= \frac{1}{2}G_{Pilot}(f) + \frac{1}{2}G_{Data}(f) \\ &= \frac{10}{11}G_{BOC(1,1)}(f) + \frac{1}{11}G_{BOC(6,1)}(f) \end{aligned} \quad (7)$$

Yet another option for a signal with 50%/50% power split between pilot and carrier component would be to place 1/11 BOC(1,1) spreading symbols on both the pilot and data, yielding the PSDs

$$\begin{aligned} G_{Pilot}(f) &= \frac{10}{11}G_{BOC(1,1)}(f) + \frac{1}{11}G_{BOC(6,1)}(f) \\ G_{Data}(f) &= \frac{10}{11}G_{BOC(1,1)}(f) + \frac{1}{11}G_{BOC(6,1)}(f) \\ G_{MBOC(6,1,1/11)}(f) &= \frac{1}{2}G_{Pilot}(f) + \frac{1}{2}G_{Data}(f) \\ &= \frac{10}{11}G_{BOC(1,1)}(f) + \frac{1}{11}G_{BOC(6,1)}(f) \end{aligned} \quad (8)$$

Several considerations affect the choice of specific locations for the BOC(6,1) spreading symbols. If BOC(6,1) symbols are placed in both the pilot and data components, receiver implementation is simplest when these symbols are placed in the same locations in both components. Also, it has been determined that proper placement of the BOC(6,1) symbols can lead to improvement of the spreading codes' autocorrelation and crosscorrelation properties, compared to these properties with all BOC(1,1) spreading symbols.

Work is underway to determine the best placement of BOC(6,1) symbols in a L1 OS signal, accounting for these considerations. Good results have been obtained for L1C using the BOC(6,1) locations shown in Fig. 3, and the resulting performance of spreading codes for L1C are reported later in this paper.

CBOC Implementation

A CBOC implementation can be based on the approach presented in [6, 9, 11], using four-level spreading symbols formed by the weighted sum of $g_{BOC(1,1)}(t)$ and $g_{BOC(6,1)}(t)$ symbols. For a 50%/50% power split between data and pilot components, CBOC symbols formed from the sum of $\sqrt{10/11}\ g_{BOC(1,1)}(t)$ symbols and $\sqrt{1/11}\ g_{BOC(6,1)}(t)$ symbols could be used on both components, yielding the PSDs in (8). Alternatively, for the same 50%/50% power split between data and pilot components, CBOC symbols formed from the sum of $\sqrt{9/11}\ g_{BOC(1,1)}(t)$ symbols and $\sqrt{2/11}\ g_{BOC(6,1)}(t)$ symbols could be used on only the pilot component, with the data component remaining all $g_{BOC(1,1)}(t)$. The resulting PSDs would be the same as (7).

The normalized autocorrelation function of the TMBOC(6,1,4/33) spread spectrum time series, computed over infinite bandwidth and with ideal spreading codes, is illustrated in Fig. 4, along with the autocorrelation function for BOC(1,1). Observe that TMBOC(6,1,4/33)'s correlation function peak is narrower than that of BOC(1,1), but the widths at values of 0.5 and at the zero crossing are virtually the same.

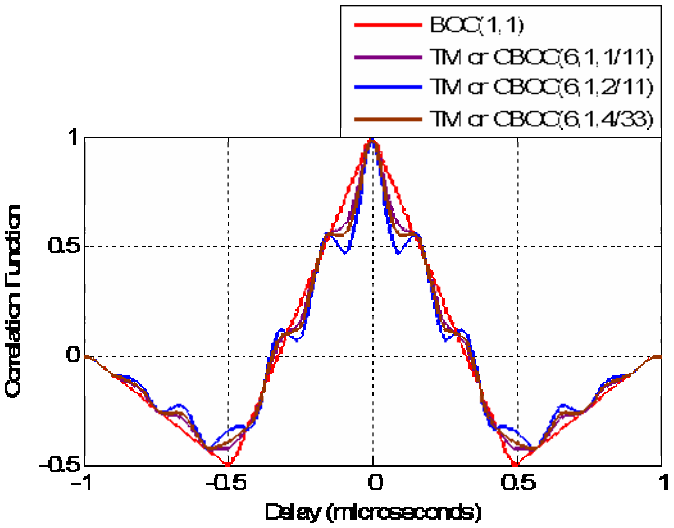

Fig. 4. Normalized Autocorrelation Functions Computed over ±15 MHz Bandwidth

Summary of Spreading Time Series and Implementation

Table 1 summarizes the variety of implementations of MBOC(6,1,1/11) that have been outlined:

Table 1. MBOC(6,1,1/11) Possible implementations

Data	Pilot	Percentage on pilot
BOC(1,1)	TMBOC(6,1,2/11)	50%
BOC(1,1)	TMBOC(6,1,4/33)	75%
TMBOC(6,1,1/11)	TMBOC(6,1,1/11)	50%
TMBOC(6,1,1/11)	TMBOC(6,1,1/11)	75%
BOC(1,1)	CBOC(6,1,2/11)	50%
BOC(1,1)	CBOC(6,1,4/33)	75%
CBOC(6,1,1/11)	CBOC(6,1,1/11)	50%
CBOC(6,1,1/11)	CBOC(6,1,1/11)	75%

PERFORMANCE ASSESSMENT

Many different performance characteristics have been considered during waveform optimization. The primary objective has been to improve tracking performance in multipath. In addition, other characteristics have also been considered, including code tracking, initial synchronization for acquisition, spreading code performance, and losses for narrowband receivers.

Multipath Performance

Since performance in multipath involves a combination of signal design and receiver processing, several different processing approaches have been considered. Furthermore, since new ideas for multipath mitigation processing are emerging, signal characteristics that appear to benefit these advanced multipath mitigation techniques are also considered.

Multipath Performance with Noncoherent Early-Late Processing

Evaluation of early-late processing performance is based on a static model with one direct and one reflected path, with a multipath to direct path signal power ratio (MDR) that is independent of delay. This model does not provide for the probability distribution of (reflected) path delay or the attenuation associated with each delay value. The results shown here employ a MDR of –6 dB. The receiver is assumed to have a four- or six-pole Butterworth band-limiting filter with –3 dB points at the stated bandwidth (BW). The filter is assumed to be phase-equalized so that the group delay is constant. Non-coherent early-late processing (NELP) is employed.

The results are provided as pairs of graphs for each combination of receiver processing parameters and different signals. The first graph is an error envelope showing maximum and minimum bias error (computed over all relative phases between the multipath and the direct path), for each delay. Many of these error envelopes have oscillatory components. The second graph is of the so-called running error. This is computed from the area enclosed within the multipath error envelope and averaged over the range of multipath delays from zero to the plotted delay values.

Fig. 5 shows the multipath error envelope for the receiver configuration of most interest, with 24 MHz pre-correlation (double-sided) bandwidth and narrow early-late spacing of $\Delta\tau$=24.4 nsec, corresponding to a fraction d=0.025 of a 1.023 MHz spreading code chip period. Fig. 6 shows the corresponding running average error, showing that both MBOC waveforms provide typically smaller average errors than either BOC(1,1) or BOC(2,2) waveforms. One of the waveform options, TMBOC(6,1,4/33), shows an average error less than those of any other option for all delays. An important feature of all the MBOC waveforms is that the error envelope diminishes at smaller path length delay values than for BOC(1,1) or BOC(2,2). At longer path length delay values, the MBOC waveforms provide lower average delays similar in value to that of a BOC(2,2) spreading symbol.

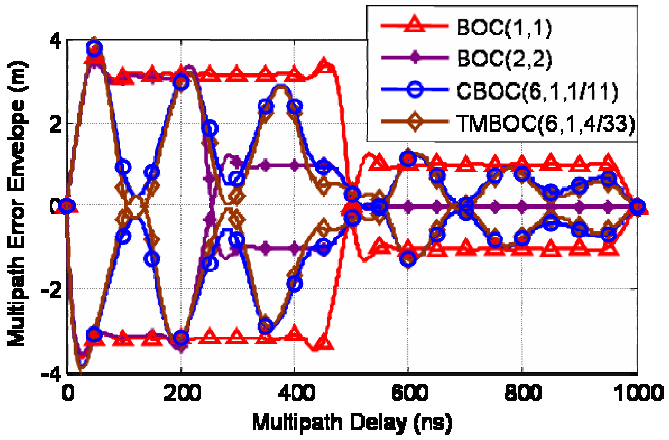

Fig. 5. Multipath Error Envelope for NELP Processing, BW=24 MHz (4 pole Butterworth), $\Delta\tau$=24.4 nsec

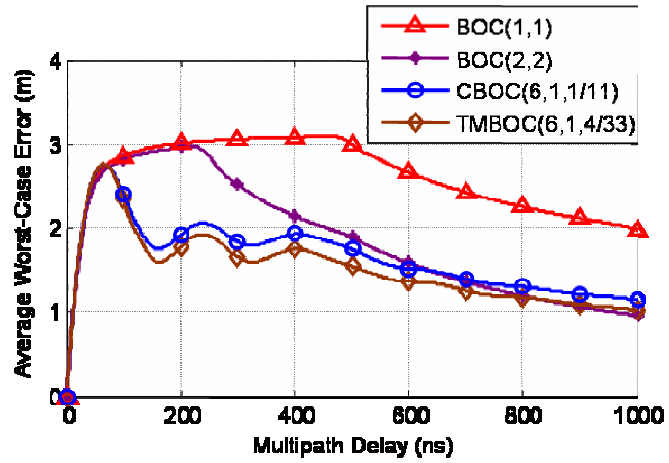

Fig. 6. Average Error for NELP Processing, BW=24 MHz (4 pole Butterworth filter), $\Delta\tau$=24.4 nsec

Fig. 7 and Fig. 8 show the corresponding results for 24 MHz precorrelation bandwidth, with a narrower early-late spacing $\Delta\tau$=12 ns, corresponding to d=0.0125 (proportion of a spreading code interval). In these figures, the multipath error envelope for a BPSK-R(10) spreading modulation has also been provided. Note that the MBOC spectrum provides error envelopes that are smaller than those for BPSK-R(10) for the small values of path length delays (less than ~120 nsec). This is the range of delays that are most common in many urban environments and have lower values of attenuation (typically less than 20-30 dB).

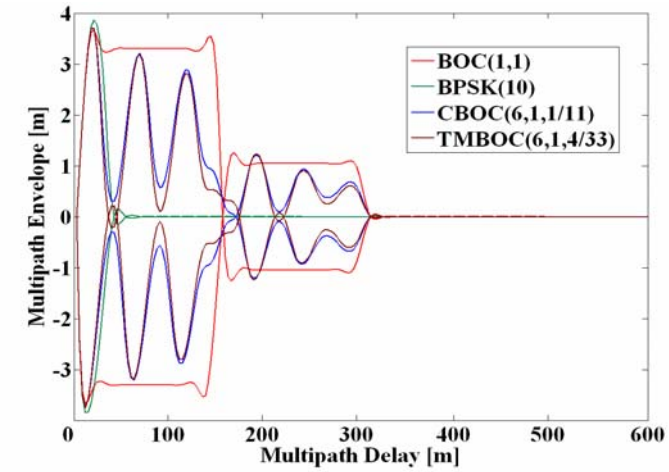

Fig. 7. Multipath Error Envelope for NELP Processing, W=24 MHz (6 pole Butterworth filter), d=0.0125 chips

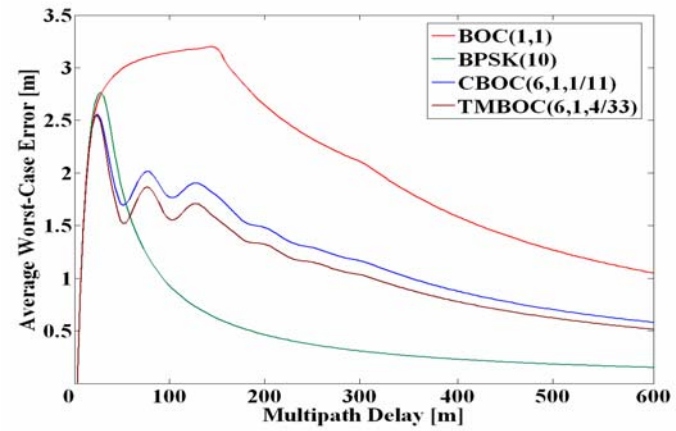

Fig. 8. Average Error for NELP Processing, BW=24 MHz (6 pole Butterworth filter), d=0.0125 chips

Fig. 9 and Fig. 10 show results for BW=24 MHz, with early-late spacing of $\Delta\tau$=48.9 nsec (d=0.05). The running average error of the MBOC waveforms are typically smaller than those for the BOC(1,1) or BOC(2,2) options. The error envelope for the MBOC(6,1,4/33) waveforms (TMBOC or CBOC) is smaller than for all other options.

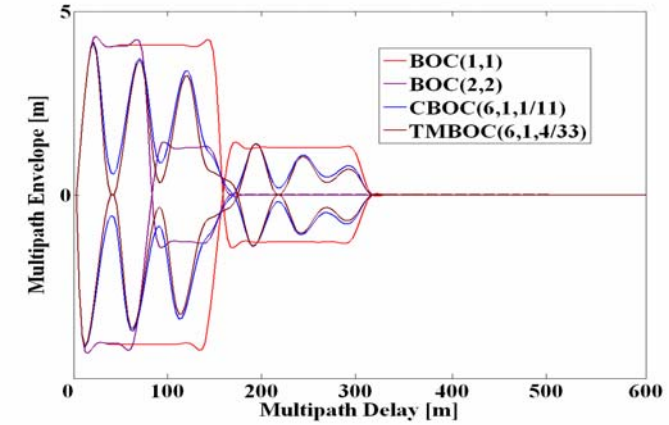

Fig. 9. Multipath Error Envelope for NELP Processing, BW=24 MHz (6 pole Butterworth filter), d=0.05 chips

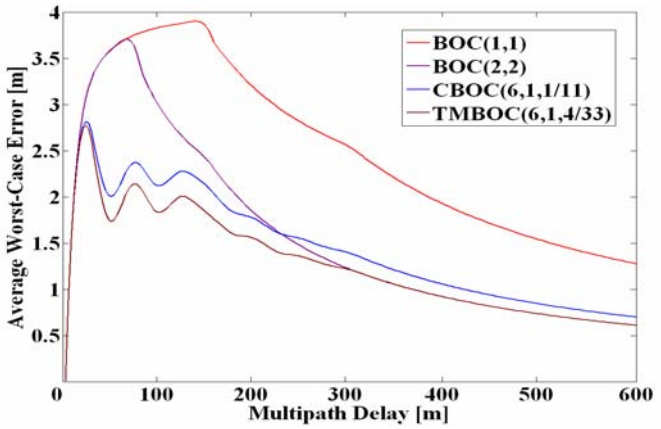

Fig. 10. Average Error for NELP Processing, BW=24 MHz (6 pole Butterworth filter), d=0.05 chips

Fig. 11 and Fig. 12 show corresponding results for a narrower BW=12 MHz, with $\Delta\tau$=48.9 nsec (d=0.05 chips). The average error of the CBOC and TMBOC waveform options are typically smaller than those for BOC(1,1) or BOC(2,2). The average errors for TMBOC or CBOC(6,1,4/33) are smaller than those for any other choice for all multipath delays.

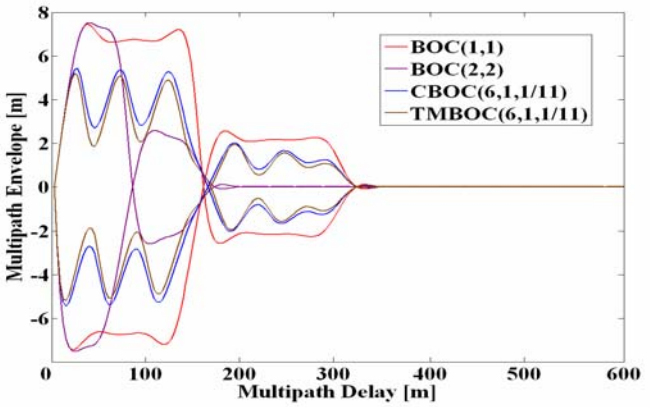

Fig. 11. Multipath Error Envelope for NELP Processing, BW=12 MHz (6 pole Butterworth filter), d=0.05 chips

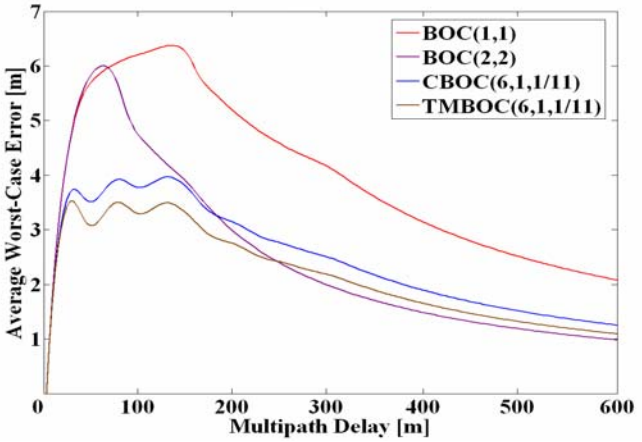

Fig. 12. Average Error for NELP Processing, BW=12 MHz (6 pole Butterworth filter), d=0.05 chips

The results for narrow correlator processors show that TMBOC(6,1,4/33) provides slightly smaller errors than for the CBOC(6,1,1/11) spreading symbol. This indicates that there is an advantage in placing all the BOC(6,1) spreading symbols in the pilot for certain applications. In every case examined, the average errors for TMBOC(6,1,4/33) and CBOC(6,1,1/11) are smaller than those for BOC(2,2) for all delays.

Multipath Performance with Double-Delta Processing

Like early-late processing, double-delta multipath mitigation processing is a known processing technique that was designed for BPSK-R spreading modulations, but may be applied to more advanced modulations as well. The double-delta technique considered in this section processes every edge. Smaller multipath error envelopes may be obtained from TMBOC and CBOC options by masking the BOC(6,1) spreading symbols in the receiver replica, so that only BOC(1,1) symbols are processed. This resulting code tracking SNR after this masked symbol replica (MSR) processing, when compared to the code tracking SNR that would be obtained from an all BOC(1,1) pilot, would be a fraction of a dB (0.4, 0.6, or 0.9 dB, depending upon time series implementation) lower. The difference in tracking error would be very small compared to other error sources, and all spreading symbols would be used for data demodulation and carrier tracking, thus making use of all the available power.

Fig. 13 and Fig. 14 show the multipath errors resulting from double-delta processing with the same multipath propagation model used previously. In these figures, the BW=24 MHz, outer early-late spacing of 48.9 nsec, and inner early-late spacing of 24.4 nsec. With MSR processing, the multipath error envelopes for the MBOC options are the same as those for BOC(1,1), whilst those from BOC(2,2) are consistently larger. The multipath errors from double-delta processing are much smaller than those from early-late processing.

Performance of Advanced Multipath Processing

A variety of advanced multipath mitigation techniques are evolving to provide improved performance. It is expected that further advances will be possible with new forms of spreading modulations. There is no specific metric which provides for the comparison of signals for advanced mitigation techniques, we have considered two. The first of these is the root-mean square (RMS) bandwidth of the spreading symbol, defined by

$$BW_{rms}(f_{\lim}) = \sqrt{\int_{-\frac{f_{\lim}}{2}}^{+\frac{f_{\lim}}{2}} f^2 \cdot \hat{G}(f) \cdot df} \qquad (9)$$

where $\hat{G}(f)$ is normalized for unit power over the signal bandwidth being used, and $f_{\lim}$ is the double sided receiver pre-correlation bandwidth.

Figure 15 shows the RMS bandwidth of the four spreading modulations for a given receiver bandwidth assumed to have rectangular bandwidths. The RMS bandwidths for the TMBOC and CBOC options are the same or larger than the RMS bandwidth for BOC(1,1) for all signal bandwidths, and larger or almost as large as those for BOC(2,2) for signal bandwidths greater than approximately 12 MHz. (High-performance receivers would be expected to use bandwidths much greater than 12 MHz.)

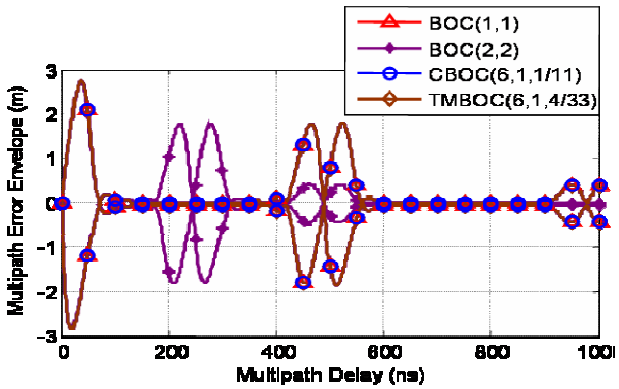

Fig. 13. Multipath Error Envelope for Double-Delta Processing, BW=24 MHz (4 pole Butterworth filter), Early-Late Spacings of 24.4 nsec and 48.9 nsec

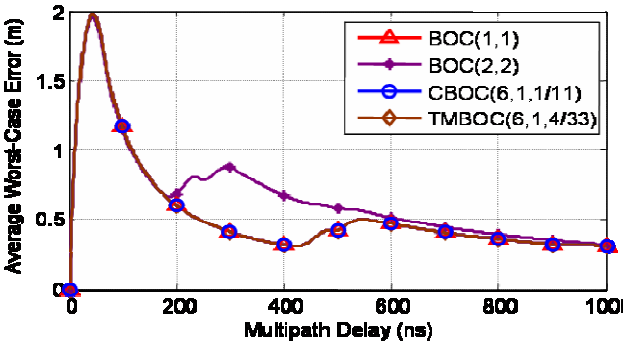

Fig. 14. Average Error for Double-Delta Processing, BW=24 MHz (4 pole Butterworth filter), Early-Late Spacings of 24.4 nsec and 48.9 nsec

Using a bandwidth of 12 MHz with one of the MBOC signal options would provide greater RMS bandwidth than using a 24 MHz bandwidth with BOC(1,1). If receivers use bandwidths less than approximately 12 MHz, they would lose a fraction of a dB of signal power with TMBOC or CBOC, compared to BOC(1,1).

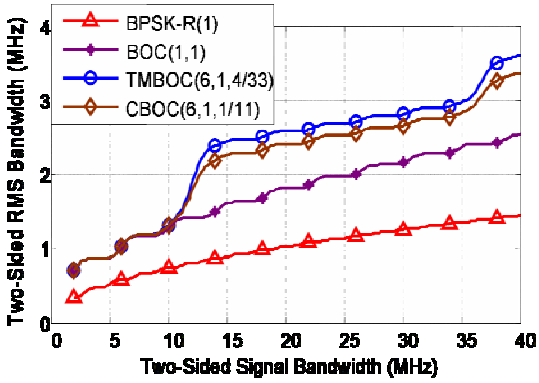

Fig. 15. RMS bandwidth vs. two-sided receiver bandwidth

A second measure of performance for advanced multipath mitigation is the number of waveform transitions in a code repeat interval. These are affected by the spreading symbol rate, the carrier offset frequency and the organization of the BOC(6,1) and BOC(1,1) components. A detailed analysis of this will not be given here. However, for the various options considered here, there is a gain of between 2.0 dB and 3.5 dB depending upon the specific waveform implementation used.

Summary of Multipath Performance

The multipath performance metrics indicate that TMBOC and CBOC options can be processed to obtain smaller multipath errors than BOC(1,1) for early-late processing. For the double-delta processor, the multipath errors for the proposed spreading symbol waveforms are the same as for BOC(1,1) and better than BOC(2,2). Both TMBOC and CBOC waveforms provide better potential for advanced multipath mitigation processing than BOC(1,1).

Spreading Code Performance

The new L1 GALILEO OS and GPS L1C spreading code family members have been designed for reduced side-lobe levels in auto- and cross-correlation functions.

One of the metrics used to select the BOC(1,1) and BOC(6,1) spreading symbols as waveform partners [13] is that these are orthogonal. This can be used to improve the auto- and cross-correlation performance. Therefore part of the design process for TMBOC implementations will be to select the locations in the code sequence where BOC(6,1) spreading symbols are placed. Judicious placement introduces zeros into the correlations at certain delays, providing a unique opportunity for additional control over the correlation functions.

The first results of this joint design of TMBOC placement and spreading codes has been completed for L1C. The pattern of BOC(6,1) spreading symbols is as shown in Fig.3. The sidelobe levels for crosscorrelations between L1C pilot codes, using the original codes selected for BOC(1,1) spreading modulations, and a different set of codes from the same family selected for TMBOC are shown in Fig. 16. The results are calculated using both even and odd crosscorrelations. Compared to the baseline spreading codes, the maximum crosscorrelation level is reduced by 0.1 dB, and its probability of occurrence is reduced by a factor of 40. The sidelobe levels at somewhat higher probability of occurrence are reduced by more than 1 dB. Similar improvements are evident in Fig. 17 for the autocorrelation sidelobes.

Performance of Low-End Receivers

GPS L1C and GALILEO L1 OS signals are being designed to benefit receivers that will make use of technology advances to attain better performance, while continuing to support receivers designed for minimal complexity. For example, receivers that employ modest bandwidths and only use the BOC(1,1) spreading symbols may offer lower cost and

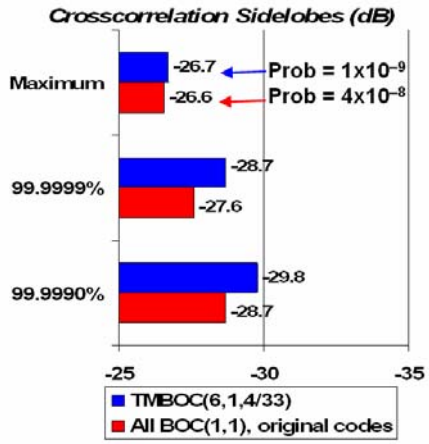

Fig. 16. Comparison of Crosscorrelation Sidelobes for L1C

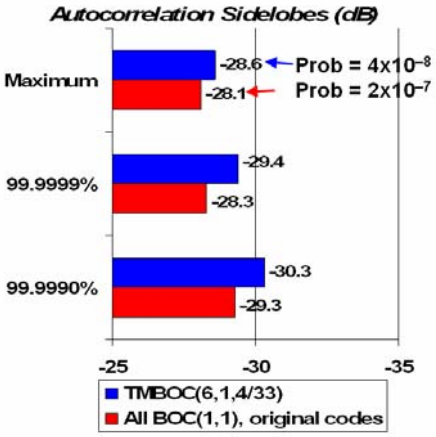

Fig. 17. Comparison of Autocorrelation Sidelobes for L1C

provide long battery life. The minimum double sided pre-correlation bandwidth for a BOC(1,1) spreading symbol is approximately 4 MHz – about twice that required for a C/A code receiver [BPSK-R(1)]. For maximum multipath mitigation performance, the widest pre-correlation bandwidth provides the best performance. The BOC(6,1) component improves the signal to noise ratio for multipath processing by up to 3.5 dB. For intermediate receiver precorrelation bandwidths, the new signals continue to provide equal or better performance than BOC(1,1) signals and near those available from a BOC(2,2) spreading symbol. Compared to BOC(1,1), the MBOC options provide almost the same performance (within 0.4, 0.6, or 0.9 dB of power, depending upon spreading time series implementation) to low-end receivers.

Radio Frequency Compatibility

Since MBOC places more power at higher frequencies, it also provides some additional benefits in radio frequency compatibility. Compared to BOC(1,1), the MBOC(6,1,1/11) spectrum has 0.7 dB less self-interference, and 0.3 dB less interference to C/A code and SBAS receivers.

SUMMARY AND WAY AHEAD

This paper has described the optimized MBOC spreading modulation recommended for GALILEO L1 OS and GPS L1C. The MBOC design continues the trend in most modernized signal designs to provide more power at higher frequencies (away from the center frequency) in order to improve code tracking and some aspects of multipath performance. MBOC does this by adding a small fraction of BOC(6,1) spectrum to the BOC(1,1) spectrum.

Since BOC(1,1) already has more high frequency power than C/A code's BPSK-R(1) spreading modulation, it already provides performance benefits over BPSK-R(1). MBOC provides additional benefits over BOC(1,1) including code tracking in noise and multipath (when using early-late processing and advanced multipath mitigation techniques), better spreading code performance than the baseline L1C codes, less self-interference, better RF compatibility with C/A, and less susceptibility to narrowband interference at the worst-case frequency. These improvements are obtained through the use of slightly more power at high frequencies, and receivers with very narrow front-end bandwidths do not obtain these benefits or use this signal power. Also, multipath mitigation techniques like double-delta processing perform better with BPSK-R(1) than with MBOC or BOC(1,1) for receivers with narrower bandwidths. Thus, BPSK-R(1), BOC(1,1), and MBOC provide different opportunities to trade performance against support for simple receiver designs.

MBOC maintains compatibility with BOC(1,1) receivers, since more than 90% of the power remains available to BOC(1,1) receivers. Like BOC(1,1), MBOC provides good potential interoperability between GPS and GALILEO, with greater interoperability and compatibility achieved if the same time waveforms and spreading code families can be employed.

Several different waveform options exist and can produce the same MBOC(6,1,1/11) power spectral density, and evaluation of these different implementation options is continuing. The final choice between BOC(1,1) and MBOC as the common spreading modulation for L1 OS and L1C awaits an assessment of programmatic aspects.

ACKNOWLEDGMENTS

The work of the European Commission Signal Task Force was supported by many European national space agencies including Deutsches Zentrum für Luft- und Raumfahrt (DLR, Germany), Centre National d´Etudes Spatiales (France), and Defence Science and Technology Laboratory (United Kingdom). Many other members of the European Commission GALILEO Signal Task Force have also contributed to this work, in particular Lionel Ries, Antoine DeLatour and Laurent Lestarquit from CNES. Their support and contribution is acknowledged.

MITRE's work was supported by the United States Air Force under contract FA8721-04-C-0001 and by the Federal Aviation Administration under contract DTFA01-01-C-00001. Work by Thomas Stansell was supported by the United States Air Forces under contract number FA8802-04-C-0001 with The Aerospace Corporation.

REFERENCES

[1] http://pnt.gov//public/docs/2004-US-EC-agreement.pdf

[2] http://gps.losangeles.af.mil/engineering/icwg/Docs/EC%20and%20US%20Joint%20Statement%20on%20GALILEO%20and%20GPS%20Signal%20Optimization%20-%20%2024%20Mar%2006.pdf

[3] http://gps.losangeles.af.mil/engineering/icwg/Docs/WGA%20Signed%20Recommendation%20on%20MBOC%20-%2023%20Mar%2006.pdf

[4] Betz, J. W., (2002), "Binary Offset Carrier Modulations for Radionavigation," *NAVIGATION: Journal of The Institute of Navigation* Vol. 48, No. 4, Winter 2001/02.

[5] Betz J. W. et al. (2002), "Candidate Design for an Additional Civil Signal in GPS Spectral Bands," *Proceedings of ION NTM 2002* - 28-30 January, 2002 - San Diego, CA

[6] Pratt, A. R et al. (2003), "Performance of GPS GALILEO Receivers Using m-PSK BOC Signals", *Proceedings of ION 2003* – 9-12 September 2003, Portland, Oregon, USA

[7] Hegarty, C. J. et al. (2004), "Binary Coded Symbol Modulations for GNSS," *Proceedings of ION-AM-2004*, 7-9 June 2004, Dayton, Ohio,USA.

[8] Hein, G. W. et al. (2005), "A candidate for the GALILEO L1 OS Optimized Signal", *Proceedings of ION GNSS 2005* – 13-16 September 2005, Long Beach, California, USA

[9] Avila-Rodriguez, J.A. et al. (2005), "Revised Combined GALILEO/GPS Frequency and Signal Performance Analysis", *Proceedings of ION GNSS 2005* – 13-16 September 2005, Long Beach, California, USA.

[10] Wallner S. et al (2005), "Interference Computations between GPS and GALILEO", *Proceedings of ION GNSS 2005* – 13-16 September 2005, Long Beach, California, USA

[11] Pratt, A. R. et al. (2006), "Tracking Complex Modulation Waveforms – How to avoid Receiver Bias", *Proceedings of IEEE/ION PLANS 2006* – 24-27 April 2006, San Diego, California, USA.